Development of a Multi-Degree-of-Freedom Ultrasonic Motor Using Single Mode Vibrations

Kayo Otokawa, Kenjiro Takemura, Takashi Maeno

Department of Mechanical Engineering, Keio University, Tokyo Institute of Technology
fr000555@hc.cc.keio.ac.jp

Abstract

This paper presents a novel type of ultrasonic motor that can generate a multi-degree-of-freedom (MDOF) movement based on a selection of reciprocating vibration modes. Ultrasonic motors driven by a single phase are more practical than those driven by dual phases. However, a single ultrasonic motor driven by a single phase cannot cause a MDOF movement. Hence, a MDOF ultrasonic motor composed of plural vibrators using a single vibration mode is designed. First, its principles are proposed. Second, the form of the vibrators and the position of the protrusions are designed using piezoelectric analysis. And then, the driving characteristics of this MDOF ultrasonic motor are measured through experiments, and are compared with simulation. As a result, it is shown that making a novel type of MDOF ultrasonic motor with a very simple form which is easy to manufacture is possible.

1. Introduction

Today, the accuracies of the IT devices, the mechanical devices, and optic devices are advanced. Based on this, small and high-precision actuators are needed. In addition, robots are being miniaturized in the pursuit of generating human-like motion. Following this, it is necessary to develop actuators that can generate dexterous, precise motion. The volume and weight of existing electromagnetic motor is large, and one electromagnetic motor can only generate single degree of freedom movement. In recent years, ultrasonic motors are attracting attention as a new type of actuator well suited for MDOF actuation. For example, Toyama developed a spherical ultrasonic motor in which three or four ring-shaped vibrators are arranged around a spherical rotor [1]. Takemura proposed a bar-shaped ultrasonic motor capable of generating three-DOF motion [2]. These motors offer silent motion and high torque. Generally, ultrasonic motors can be divided into two types, either driven by a single phase and by dual phases. Ultrasonic motors driven by dual phases are high in efficiency and can easily reverse rotation. However, they requires much time and cost to manufacture, because their frequencies must correspond. Thus, an ultrasonic motor using plural vibrators, each vibrator is driven by a single phase is developed [3]. However, it is complex form and can not generate complex movements. In this study, we propose an ultrasonic motor which is simple form and can generate complex movements. It has four vibrators each one is driven by a single vibration mode. A spherical rotor can rotate on three perpendicular axes. The form of the vibrator and its vibration modes are designed using finite element analysis. In addition, the driving characteristics of this developed motor are also measured.

2. Design

2.1. Principles

Fig. 1 shows the structure of the developed MDOF ultrasonic motor. This ultrasonic motor is composed of four vibrators and a spherical rotor. Each vibrator is driven by an independent single vibration mode. Therefore, coupling frequencies and reprocessing is unnecessary. This mechanism realizes an ultrasonic motor with a very simple form and is easy to manufacture. As shown in Fig. 2, the protrusion placed between the loop and node of a standing wave generates rectilinear reciprocating motion. From this motion, each vibrator generates the frictional force on the rotor. The rotor is driven by the total force. In addition, each vibrator has three patterns of vibration modes that can be changed by adjusting frequencies. When these vibration modes are selected appropriately, the rotor can be rotated on three axes by combining these vibration modes. Furthermore, changing the own frequency of each vibrator can control rotational directions.

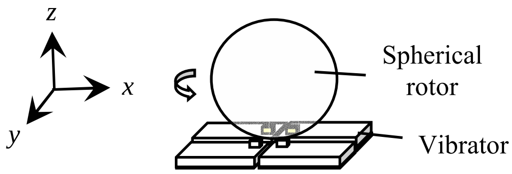

Figure 1: Structure of MDOF ultrasonic motor

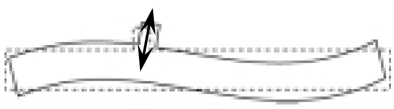

Figure 2: Motion of the protrusion

2.2. Piezoelectric Analysis

Fig. 3 shows the form of a vibrator. It is made up of a 16mm × 14mm × 1.5mm stainless-steel plate which has a 1 cubic millimeter protrusion and 0.5mm thick piezoelectric ceramic (PZT) plate with the base divided into four electrodes. Each vibrator maintains contact with the rotor at a single point of the protrusion. Both the dimension of the vibrators and the position of the protrusions were designed through piezoelectric analysis. We used finite element code ANSYS, and analyzed natural frequencies, natural vibration modes, and vibration directions of the contact point. The dimension which fulfills all the design conditions was found as shown in Fig. 3. Fig. 4 shows the vibration modes used to drive the motor. Fig. 4 (a), (b), and (c) show mode 1, 2, and 3, respectively. The protrusion is placed where it is to output force in three directions.

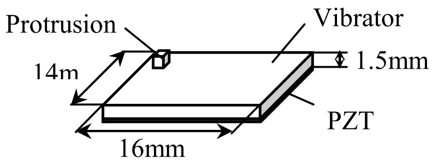

Figure 3: Form of the vibrator

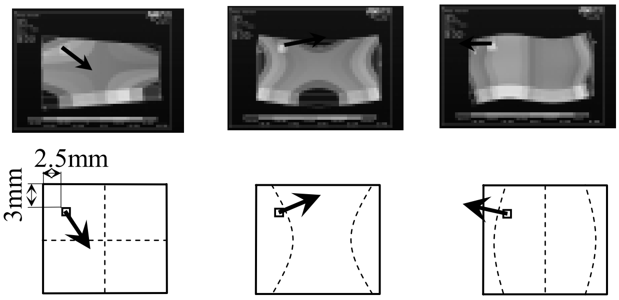

(a) Mode 1 (b) Mode 2 (c) Mode 3

Figure 4: Vibration modes

Table 1: Natural frequencies

Vibration Mode	Calculated Natural Frequency [kHz]	Measured Natural Frequency [kHz]
Mode 1	21.816	22.347
Mode 2	31.352	31.530
Mode 3	88.012	86.320

Table 2: Calculated vibration angles

Vibration Mode	Calculated Vibration Angle θ [deg]
Mode 1	47.6
Mode 2	20.0
Mode 3	26.4

The calculated natural frequencies of each vibration mode using piezoelectric analysis are shown in Table 1. The differences between each frequency can be considered to be large enough. Thus, the correct vibration mode was excited. Table 2 shows vibration angles θ of the contact point at each vibration mode.
The definition of the angle θ is shown in Fig. 5. θ is the angle between vibration direction and contact surface. The rotor is stainless-steel ball 40mm in diameter, and sustained by four points. Fig. 6 shows the combination of vibration modes. The rotation on *x*-axis is driven by the mode 2 and mode 3, as shown in Fig. 6 (a). The rotation on *y*-axis is driven by the mode 1 and mode 2, as shown in Fig. 6 (b). The rotation on *z*-axis is driven by the mode 2 and mode 3, as shown in Fig. 6 (c). Fig. 7 shows the manufactured motors. Fig. 7 (a) shows a single vibrator. Five lead wires are connected to the vibrator. One is attached to the top surface as ground and the others are pasted to each electrode. Fig. 7 (b) shows the layout. The rotor is placed on the vibrators as shown in Fig. 7 (c).

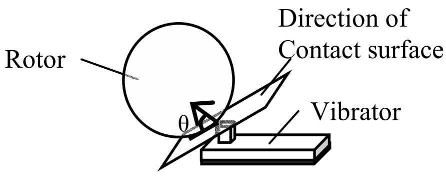

Figure 5: Definition of vibration angle θ

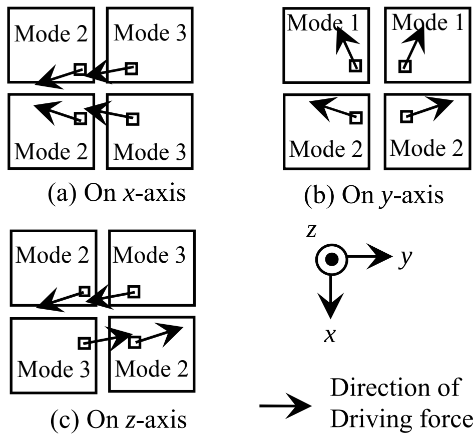

Figure 6: Combination of vibration modes

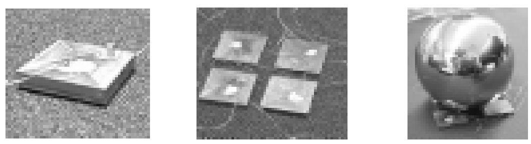

(a) Vibrator (b) Layout (c) Overall view

Figure 7: Manufactured motor

2.3. Layout of PZT

By placing a layer of PZT where the strain is large, the desired natural vibration modes can be efficiently excited. Therefore, we examined the strain distribution of the vibrator when each vibration mode was excited. The results are shown in Fig. 8. To excite all desired vibrations, a layer of PZT was located on the whole underside of the stainless-steel plate, and was divided into quarters. Putting this into consideration, excitation patterns were decided as shown in Fig. 9. Vibration can efficiently be excited by applying voltage according to these patterns. Furthermore, one of the four electrodes is used as the sensor field. This sensor field detects the amplitude of the vibrator quantitatively.

3. Measurements

3.1. Frequency Response

The natural frequencies of the vibrators were measured using an impedance gain phase analyzer. The measured natural frequencies are shown in Table 1. According to Table 1, the analysis results and the measurements are about the same. The admittance loops of each vibration mode are shown in Fig. 10. As shown in Fig. 10 (a), the admittance of Mode 1 is extremely small. The possible cause of this small value is that the position of the PZT was inappropriate for mode 1. Changing the input voltage according to the vibration mode should improve this problem.

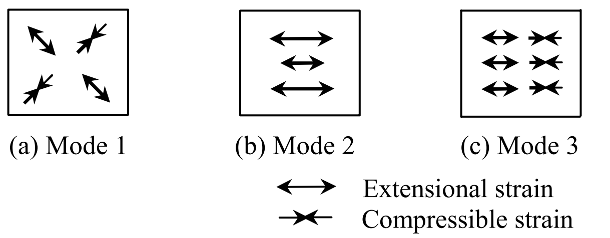

Figure 8: Strain distributions

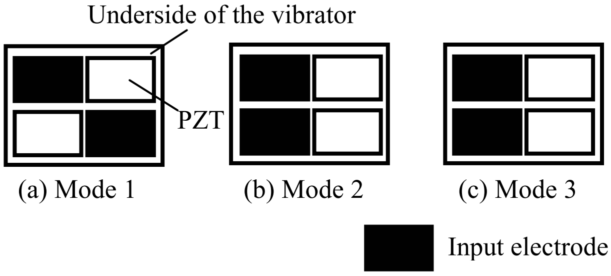

Figure 9: Excitation patterns

3.2. Vibration modes

Vibration velocity at each contact point was measured using a laser Doppler velocimeter. From the results, we calculated the amplitude of the vibration in each direction and the vibration angles θ of the contact point. Table 3 shows the vibration angles θ of the contact point. Compared with Table 2, it is confirmed that the contact point vibrates in the same direction as simulation. Thus, the validity of the model used for piezoelectric analysis is proved.

3.3. Driving Characteristics

First, we confirmed that each vibrator vibrates in the desired directions. We then also confirmed that a rotor can be rotated on three axes. The input voltages were around 100 Vp-p maximum. The maximum torque and no-load rotational speed of each rotation are shown in Table 4.

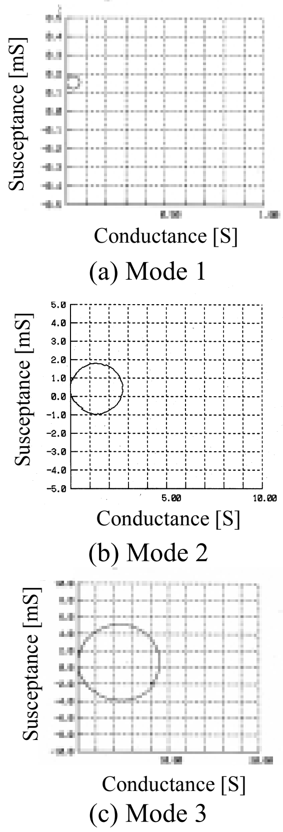

Figure 10: Admittance of each vibration mode

Table 3: Measured vibration angles

Vibration Mode	Measured Vibration Angle θ [deg]
Mode 1	45.6
Mode 2	18.6
Mode 3	24.1

Table 4: Maximum torque and no-load rotational speed

Rotation	Maximum Torque [mN-m]	No-load Rotational Speed [rpm]
On *x*-axis	15	70
On *y*-axis	4	19
On *z*-axis	5	75

The maximum torque of the rotation on the *x*-axis was about 15 mN-m. Considering principles of the developed ultrasonic motor, which is driven by rectilinear reciprocating vibration, this result seems to be relatively good. On the other hand, however, the values of the rotation on the *y*-axis are smaller than the other two. The possible cause of this is the small admittance of mode 1 and a vibration direction of mode 2. The *x*-axial component of mode 2 may have been too large that it disturbed the rotation on the *y*-axis. In order to obtain better driving characteristics of the rotation on the *y*-axis, the layout of the PZT or the vibration directions at the contact point should be reconsidered. Fig. 11 shows the torque-rotational speed curve obtained when the rotor was driven on each axis. The rotational speed decreases with the torque.

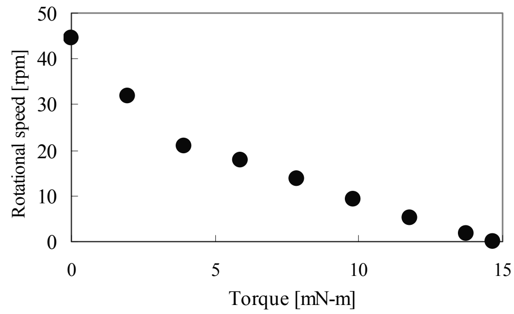

(a) On *x*-axis

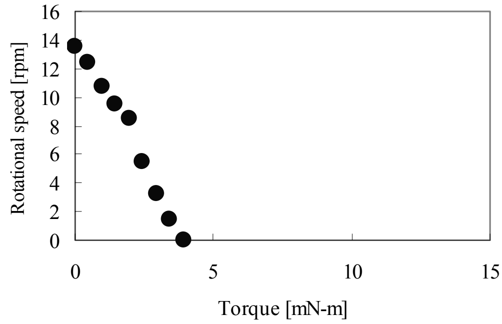

(b) On *y*-axis

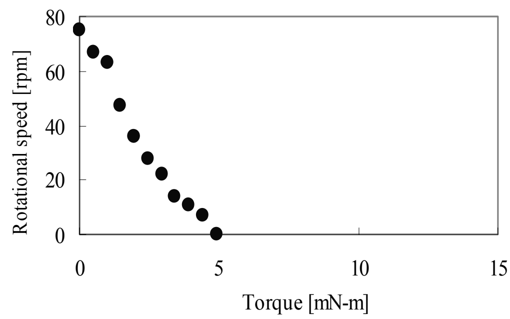

(c) On *z*-axis

Figure 11: Measured T-N curve of the motor

4. Conclusions

In this study, we proposed a MDOF ultrasonic motor driven by selecting single vibration modes. Combining single vibration modes proved effective in rotating a spherical rotor on three perpendicular axes. In addition, we measured the driving characteristics of the developed ultrasonic motor. The maximum torque of rotation on the *x*-axis was about 15 mN-m. However, maximum torque on the other axes was smaller. In order to solve this problem, the layout of PZT or the vibration directions of the contact point should be reconsidered. In the future, this ultrasonic motor will be miniaturized and be able to generate higher torque. The developed ultrasonic motor offers a wide range of applications. The form of the vibrator and rotor is changeable. In addition, it is availableness for miniaturization because of its simple form. And it is cheap to manufacture and easy to manufacture. In the future, this motor may be used for a number of applications, such as adjusting the lens on cameras, and joints of robot arms.

5. Acknowledgements

This study was supported in part by Grant-in-Aid for Encouragement of Young Scientists (B) 15760093 of the Ministry of Education, Culture, Sports, Science and Technology of Japan. Authors also would like to thank the staff of Canon Inc. for their help in manufacturing the vibrators and PZT.

6. References

[1] S. Toyama *et al.*, Development of an Actuator for a Robotic Manipulator with Ultrasonic Motor -2nd Development of Prototypal Spherical Ultrasonic Motor-, Journal of the Robotics Society of Japan, Vol. 13, No. 2, pp. 235-241, 1995

[2] K. Takemura *et al.*, Development of a Bar-shaped Ultrasonic Motor for Multi-degrees of freedom Motion, Proc. Fourth International Conference on Motion and Vibration Control, Vol. 1, 1998, pp. 195-200

[3] A. Ferreira *et al.*, Dynamic Modeling and Control of a Conveyance Microrobotic System Using Active Friction Drive, IEEE/ASME Transactions on MECHATRONICS, Vol. 8, No. 2, pp. 188-202, 2003